

Impact ionization rate in GaAs

Michael Stobbe and Ronald Redmer

Universität Rostock, Fachbereich Physik, Postfach 999, D-18055 Rostock, Germany

Wolfgang Schattke

Institut für Theoretische Physik, Christian-Albrechts-Universität Kiel,

Leibnizstraße 15, D-24118 Kiel, Germany

(Received 22 July 1993; revised manuscript received 21 October 1993)

The impact ionization rate and its orientation dependence in \mathbf{k} space is calculated for GaAs. The numerical results indicate a strong correlation to the band structure. The use of a q -dependent screening function for the Coulomb interaction between conduction and valence electrons is found to be essential. Comparison with recent results for Si, GaAs shows a harder threshold behavior. A simple fit formula is presented for easy calculation of the direction-dependent transition rate. With only the band structure as input the numerical results are closely reproduced in an arbitrary direction in the Brillouin zone.

I. INTRODUCTION

The impact ionization rate is of basic interest in understanding electron transport in semiconductors at high electric-field strengths. This microscopic quantity is necessary for calculating the probability of the electron to ionize, which is described by the ionization coefficient α . Special effects obtained for the impact ionization rate may be examined experimentally by studying the ionization coefficient. For example, several hints for an orientation dependence of α were given experimentally for Si (Ref. 1) as well as for GaAs.² More recent measurements by Bulman, Robbins, and Stillman³ indicate a more isotropic behavior of α for GaAs.

Another interesting feature is the threshold behavior. Both anisotropy and threshold behavior were intensively studied recently by several authors⁴⁻⁷.

In our earlier paper,⁸ we calculated the impact ionization rate for GaAs numerically, including a local empirical pseudopotential band structure and the corresponding wave functions. In particular, a reasonable description of the ionization rate was obtained for the high-energy range, whereas the sensitive behavior near the threshold required a more refined integration scheme extending the rather small number of special points in the Brillouin zone.

A more precise calculation of the impact ionization rate for GaAs near the threshold was performed recently by Bude and Hess.⁴ They used a Monte Carlo technique similar to that of Kane,⁹ also including a realistic band structure. They obtained a rather soft behavior, contrary to that which follows from the often-used Keldysh formula.¹⁰

Bude, Hess, and Iafrate⁵ treated the problem of the ionization rate in a more complete way, including special effects of high fields and high scattering rates, such as collision broadening and the intracollisional field effect. Following their representation both influences effect a softening of the threshold energy for the impact ionization.

A special calculation for the description of the \mathbf{k} dependence of the impact ionization rate was performed by Wang and Brennan.⁶ They considered the band struc-

ture by applying the $\mathbf{k}\cdot\mathbf{p}$ scheme. Their results give a qualitative picture of the anisotropy of the ionization rate.

Recently, Sano and Yoshii⁷ have performed an evaluation of the impact ionization rate for Si using a very efficient deterministic numerical procedure. In comparison to our former calculation, their special integration scheme takes into account a rather high number of points in the Brillouin zone, so that they were able to study effects of the anisotropy in \mathbf{k} space as well as the threshold behavior for Si. Both were found to be direct consequences of the band structure.

In this paper we investigate the impact ionization rate and its orientation dependence in GaAs. The calculation is performed using the integration method of Sano and Yoshii.⁷

Inserting band structures which are obtained from different sets of local pseudopotential parameters for GaAs, the pronounced correlation of the particular band shapes with the impact ionization rate is shown in detail. In addition, we carried out a similar calculation of the ionization rate for Si. Generally, the results for the averaged scattering rate show a distinct correlation to the density of states in these materials which causes the specific threshold behavior.

Exchange and umklapp processes are included in the evaluation of the impact ionization rate. The consideration of an appropriate wave-vector-dependent screening function for the Coulomb interaction in semiconductors is of significant influence on the results.

Details of the numerical method for the calculation of the interband transition rate are briefly outlined in Sec. II. We show the results for GaAs using various band structures in Sec. III, especially the orientation dependence, and finally compare the averaged energy-dependent values with those for Si. A summary and conclusions are given in Sec. IV.

II. THEORY AND NUMERICAL METHOD

The impact ionization rate is usually determined from Fermi's golden rule,

$$r(\mathbf{k}_1, \nu_1) = \frac{2\pi}{\hbar} \frac{\Omega^3}{(2\pi)^9} \sum_{\nu_2, \dots, \nu_4} \int \cdots \int d^3k_2 d^3k_3 d^3k_4 |M_{\text{tot}}(1, 2, 3, 4)|^2 \delta[E_{\nu_1}(\mathbf{k}_1) + E_{\nu_2}(\mathbf{k}_2) - E_{\nu_3}(\mathbf{k}_3) - E_{\nu_4}(\mathbf{k}_4)], \quad (1)$$

where Ω and ν_i are the crystal volume and the band index, respectively. M_{tot} denotes the matrix element for ionization including exchange and umklapp processes. The initial electron states belong to the conduction (1) and valence (2) bands, whereas the final ones are both in the conduction band [(3) and (4)]. The integrals are extended over the Brillouin zone. The ionization rate Eq. (1) is integrated over all directions in \mathbf{k} space to obtain an averaged, energy-dependent impact ionization rate

$$R(E) = \frac{\sum_{\nu_1} \int d^3k_1 \delta[E_{\nu_1}(\mathbf{k}_1) - E] r(\mathbf{k}_1, \nu_1)}{\sum_{\nu_1} \int d^3k_1 \delta[E_{\nu_1}(\mathbf{k}_1) - E]}. \quad (2)$$

The analytical evaluation of the transition rate¹¹ requires strongly simplifying assumptions such as a parabolic band structure and free-electron wave functions, which are not well founded for semiconductors with a direct (GaAs) or even an indirect gap (Si). Therefore, a considerable amount of effort has been centered on the development of efficient numerical methods for the evaluation of the multidimensional integrals in Eqs. (1) and (2), in order to take into account a realistic band structure and corresponding wave functions in the entire Brillouin zone. Kane⁹ first utilized the Monte Carlo method to perform these integrations for Si. However, his random sampling method assumes that the integrands are smoothly varying functions, which is possibly not fulfilled for the ionization rate in the entire Brillouin zone.

In our previous paper,⁸ we applied the special-point method¹² for the evaluation of the impact ionization rate in GaAs. Within this method, the integrals over the whole Brillouin zone are replaced by a weighted sum over values of the integrand at special points in \mathbf{k} space. Though the maximum number of special points was limited by computer capacity reasons (we actually used one-, two-, and four-point sets), the results revealed the behavior of the impact ionization rate especially for the high-energy range, i.e., for energies greater than 4 eV (see Fig. 5).

Sano and Yoshii (Ref. 7) made extensive use of symmetry relations imposed by the crystal structure, and were able to take into account a great number of points in the Brillouin zone for the evaluation of the integrations in Eq. (1) for Si. This method is accurate enough to treat even more sensitive effects such as the threshold behavior or the orientation dependence of the interband transition rate successfully.

We have calculated the band structure and wave functions within the framework of the empirical pseudopotential method,¹³

$$\Psi_{\mathbf{k}}^{\nu}(\mathbf{r}) = \frac{1}{\sqrt{\Omega}} \sum_{\mathbf{G}} \alpha_{\mathbf{G}}^{\nu}(\mathbf{k}) e^{i(\mathbf{k}-\mathbf{G})\cdot\mathbf{r}}, \quad (3)$$

where the periodic part of the (Bloch) wave function is

expanded with respect to a basis set of reciprocal-lattice vectors \mathbf{G} . First we have utilized the set of pseudopotential parameters given by Cohen and Bergstresser (Ref. 13). The expansion runs over 113 \mathbf{G} vectors to produce a reasonable band structure in the entire Brillouin zone, and especially, to give a realistic description near the threshold. A plot of the band structure is presented in Fig. 1.

The matrix element M_{tot} contains terms for direct (D) and exchange (E) processes,

$$|M_{\text{tot}}|^2 = 2|M_D|^2 + 2|M_E|^2 - |M_D^* M_E + M_D M_E^*|. \quad (4)$$

The interaction between the electrons in the bands is described by a statically screened Coulomb potential

$$V(q) = \frac{e^2}{\epsilon_0 \epsilon(q) q^2}. \quad (5)$$

The consideration of the wave-vector dependence of the dielectric function $\epsilon(q)$ is of importance for the calculation of the matrix elements in semiconductors, as pointed out already by Laks *et al.*¹⁴ For the interaction between conduction and valence electrons, we apply here a q -dependent dielectric function derived by Levine and Louie¹⁵ which has been highly successful in calculating the quasiparticle band structure of various materials, including Si and GaAs.¹⁶ This model incorporates the correct long- and short-range properties of the dielectric function and, in addition, some consequences of the presence of a gap in the excitation spectrum characteristic of semiconductors. The interaction between electrons in the conduction band can be modeled by a Debye potential

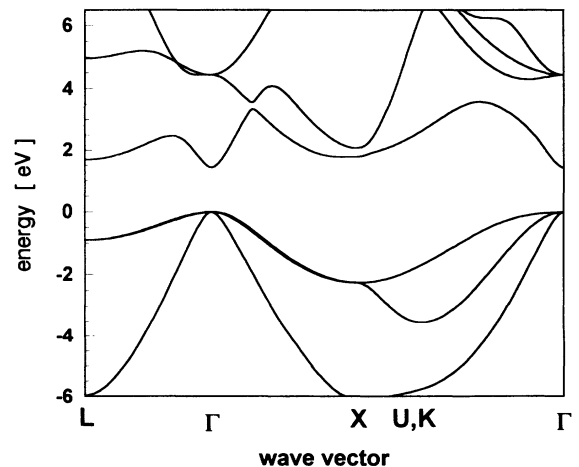


FIG. 1. Pseudopotential band structure of GaAs from Ref. 13.

with an inverse screening length $\kappa = [n_0 e^2 / (\epsilon_0 k_B T)]^{-1/2}$ for a temperature of $T = 300$ K and a corresponding electron density of $n_0 = 10^{16} \text{ cm}^{-3}$.

The \mathbf{k} vectors are restricted to the first Brillouin zone with respect to the reduced zone scheme. The momentum conservation can be expressed in general by

$$\mathbf{k}_1 + \mathbf{G}_1 + \mathbf{k}_2 + \mathbf{G}_2 = \mathbf{k}_3 + \mathbf{G}_3 + \mathbf{k}_4 + \mathbf{G}_4 .$$

Introducing the abbreviations

$$\mathbf{G}_U = \mathbf{G}_1 - \mathbf{G}_3 ,$$

$$\mathbf{G}_O = \mathbf{G}_3 + \mathbf{G}_4 - \mathbf{G}_1 - \mathbf{G}_2 ,$$

we obtain the following expression for the direct contribution to the matrix element for ionization processes:

$$\begin{aligned} |M_D|^2 &= \left| \langle \Psi_{\mathbf{k}_1}^{\nu_1} \Psi_{\mathbf{k}_2}^{\nu_2} | V(q) | \Psi_{\mathbf{k}_3}^{\nu_3} \Psi_{\mathbf{k}_4}^{\nu_4} \rangle \right|^2 \\ &= \frac{1}{\Omega^2} \left[\frac{e^2}{\epsilon_0} \right]^2 \sum_{\mathbf{G}_O} \left| \sum_{\mathbf{G}_U} \frac{B_{\nu_1 \nu_3}^{(\mathbf{G}_U)}(\mathbf{k}_1, \mathbf{k}_3) B_{\nu_2 \nu_4}^{(\mathbf{G}_O - \mathbf{G}_U)}(\mathbf{k}_2, \mathbf{k}_4)}{\epsilon(q) |q^2 + \kappa^2|} \right|^2 \delta_{\mathbf{k}_1 + \mathbf{k}_2, \mathbf{k}_3 + \mathbf{k}_4 + \mathbf{G}_O} . \end{aligned} \quad (6)$$

The term for the exchange process M_E is obtained simply by exchanging the indices for the final electron states 3 and 4. The momentum transfer is given by $\mathbf{q} = \mathbf{k}_1 - \mathbf{k}_3 + \mathbf{G}_U$, and the Bloch integrals are calculated from

$$B_{\nu, \nu'}^{(\mathbf{G})}(\mathbf{k}, \mathbf{k}') = \sum_{\mathbf{G}} \alpha_{\mathbf{G}}^{\nu}(\mathbf{k}) \alpha_{\mathbf{G} - \mathbf{G}}^{\nu'}(\mathbf{k}') . \quad (7)$$

We want to mention at this point that for umklapp processes, i.e., $\mathbf{G}_U \neq 0$ or $\mathbf{G}_O \neq 0$, we have to consider terms which go beyond the expansion up to the 113 \mathbf{G} vectors of the pseudopotential band-structure calculation. The respective expansion coefficients, i.e., those belonging to reciprocal-lattice vectors with $|\mathbf{G}| > \sqrt{20}(2\pi/a)$, were calculated by means of perturbation theory:¹⁷

$$\alpha_{\mathbf{G}}^{\nu}(\mathbf{k}) = \frac{\sum_{\mathbf{G}'} V(\mathbf{G} - \mathbf{G}') \alpha_{\mathbf{G}'}^{\nu}(\mathbf{k})}{\hbar^2 (\mathbf{k} - \mathbf{G})^2 / (2m_e) - E_{\nu}(\mathbf{k})} , \quad (8)$$

where $V(\mathbf{G})$ corresponds to the set of pseudopotentials. The values for $E_{\nu}(\mathbf{k})$ and $\alpha_{\mathbf{G}}^{\nu}(\mathbf{k})$ are determined by the pseudopotential calculation carried out at a former stage.

The numerical treatment of Eqs. (1) and (2) requires an appropriate replacement of the energy-conserving δ functions. Besides the Lorentz profile used in our earlier paper,⁸ the δ function is replaced here by rectangles of unit area with a height of $1/\delta E$ and a corresponding width of δE ,

$$\delta[E - E_{\nu}(\mathbf{k})] = \begin{cases} 1/\delta E, & |E - E_{\nu}(\mathbf{k})| \leq \delta E/2 \\ 0, & |E - E_{\nu}(\mathbf{k})| > \delta E/2 , \end{cases} \quad (9)$$

where for δE we take a value of 0.2 eV, as already chosen by Kane.⁹

It is interesting to compare the numerical details of the special-point method¹² with those of Ref. 7. Both methods are based upon a discretization of the \mathbf{k} space, and a replacement of integrals by sums over respective finite space elements. The special-point method, however, constructs *by definition* a finite set of those special points for the best approximation of the integrals over the Brillouin zone. Most of the computational time need-

ed within this method stems from the involved band-structure calculation which has to be performed for the large number of \mathbf{k} vectors contributing to the respective sums as a result of momentum conservation. Contrary to the special-point method, Sano and Yoshii (Ref. 7) used a cubic mesh of equidistant points for the discretization of the Brillouin zone. All linear combinations of those points in the Brillouin zone reproduce another point of the set utilizing the translational invariance with respect to a reciprocal-lattice vector \mathbf{G} . The momentum conservation is then realized with the chosen set only, and the corresponding wave vectors and energy values are calculated and stored in the preceding band-structure calculation.

An important feature of such methods, in general, is that the storage of energy values and wave functions can be restricted to the irreducible wedge (IW) if the symmetry properties of the Brillouin zone are fully exploited. The wave function for a wave vector $T_k \mathbf{k}$, which is obtained by operating one of the 48 transformations T_k of the lattice point group on a wave vector \mathbf{k} of the IW, is then determined from $\alpha_{\mathbf{G}}^{\nu}(\mathbf{k})$ via the relations

$$\begin{aligned} \alpha_{\mathbf{G}}^{\nu}(T_k \mathbf{k}) &= e^{i(T_k^{-1} \mathbf{G} - \mathbf{G}) \cdot \tau} \alpha_{T_k^{-1} \mathbf{G}}^{\nu}(\mathbf{k}) , \\ \alpha_{\mathbf{G}}^{\nu}(\tilde{T}_k \mathbf{k}) &= e^{i(\tilde{T}_k^{-1} \mathbf{G} + \mathbf{G}) \cdot \tau} \alpha_{\tilde{T}_k^{-1} \mathbf{G}}^{\nu*}(\mathbf{k}) , \end{aligned} \quad (10)$$

where in our convention τ is half of the distance between neighboring Ga and As atoms in the real lattice. The upper relation corresponds to a transformation T_k which changes the sign of two or no vector components of a \mathbf{k} vector in the IW, whereas the other produces an additional inversion. The global phase factor, which is obtained when applying the band-structure calculation, averages out in that calculation. The mesh in \mathbf{k} space is constructed with regard to the limits of the IW,

$$\begin{aligned} 0 \leq k_x + k_y + k_z &\leq 1.5 \left[\frac{2\pi}{a} \right] , \\ 0 \leq k_z \leq k_y \leq k_x &\leq \left[\frac{2\pi}{a} \right] , \end{aligned}$$

as well as to the condition for the interval length of the assumed grid $\Delta k_i = 1/n(2\pi/a)$, $i = \{x, y, z\}$ with $n \in \mathbb{N}$.

For the determination of the averaged ionization rate $R(E)$, we take a mesh of 152 points in the IW [$\Delta k_i = \frac{1}{10}(2\pi/a)$]. For the special study of the behavior of $r(\mathbf{k}, \nu)$ with respect to the various \mathbf{k} directions, we enlarge the set up to 356 points in the IW [$\Delta k_i = \frac{1}{14}(2\pi/a)$]. The summations over the conduction-band indices were restricted to the three lowest bands, whereas all four valence bands were taken into account.

III. RESULTS AND DISCUSSION

In order to investigate the influence of the band structure (see Fig. 1) on the ionization rate, we examine $r(\mathbf{k}_i, \nu_i)$ [Eq. (1)], especially along three symmetry lines. There are only a few points in the first conduction band that satisfy the threshold condition and, therefore, the total rate is almost due to electrons in the higher conduction bands. Concerning the anisotropy of the ionization rate of GaAs, we restrict our presentation in Figs. 2–4 to initial electron states in the second conduction band, which provide the main contributions near the threshold. The other summations run over all the bands already mentioned.

In Fig. 2 we have plotted the values of the ionization rate obtained for initial electrons in the second conduction band for \mathbf{k} points along three symmetry lines, versus the corresponding energy values given by the band structure obtained from Ref. 13. The functional correlation is obvious, and shows that the ability to excite valence electrons into a conduction band is closely connected to the energy of the initial electron, i.e., it increases with elec-

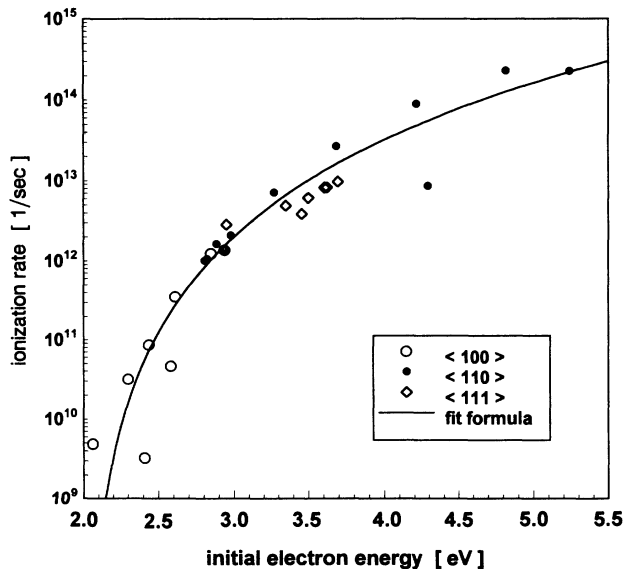


FIG. 2. Ionization rate for GaAs calculated for \mathbf{k} points along three symmetry lines plotted vs corresponding energy values given by the band structure. The fit formula [Eq. (11)] was also included.

tron energy.

Furthermore, we have added a fit including only two parameters that interpolates likewise between the points of all three directions. The number of points in the different directions is fixed by the assumed grid, and a further expansion of those would go beyond our actual computer capacity. Nevertheless, the fitted functional correlation enables us to calculate the ionization rate at each \mathbf{k} point of the Brillouin zone. The deviations of some points may be due to a slightly more complicated functional correlation. Furthermore, other band structures can lead to a different fit formula, as we observed using the band structure of Humphries and Srivastava.¹⁸

To find out which part of Eq. (1) is the main source of the distinct correlations, we first examined separately the dependence of the matrix elements on the direction of the initial electron in \mathbf{k} space. In agreement with the results of Ref. 7 for Si, we have found that the matrix elements are almost isotropic. This result confirms the assumption

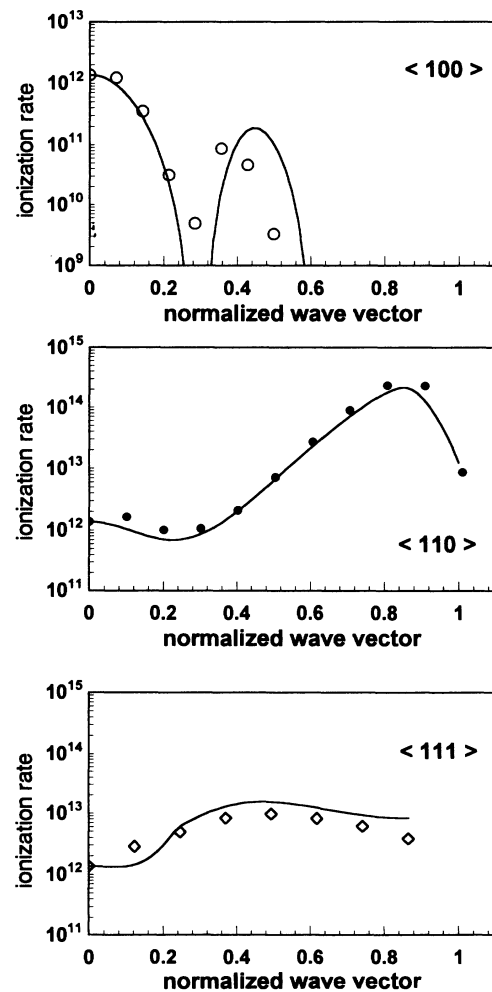


FIG. 3. Ionization rate (in sec^{-1}) for GaAs obtained from the present numerical calculation (open circles) and from the fit formula of Eq. (11) along the (a) $\langle 100 \rangle$, (b) $\langle 110 \rangle$, and (c) $\langle 111 \rangle$ directions.

that the anisotropy of the ionization rate is caused mainly by energy and momentum conservation and, especially, is determined by the initial electron energy. The slightly different functional correlation for different directions may be due to the interdependence between energy conservation, momentum conservation, and the available phase space.

The simple fit formula in Fig. 2 can be given by an expression

$$\bar{\tau}(\mathbf{k}_1, v_1) = P[E_{v_1}(\mathbf{k}_1) - E_{th}]^a, \quad (11)$$

where the parameters are fixed to $P = 2 \times 10^{12} \text{ s}^{-1} \text{ eV}^{-a}$, and $a = 4$. The threshold energy was determined to be $E_{th} = 2.1 \text{ eV}$ (see Fig. 5).

In Fig. 3, the approximate ionization rate $\bar{\tau}(\mathbf{k})$ obtained by applying the above fit formula is compared to values

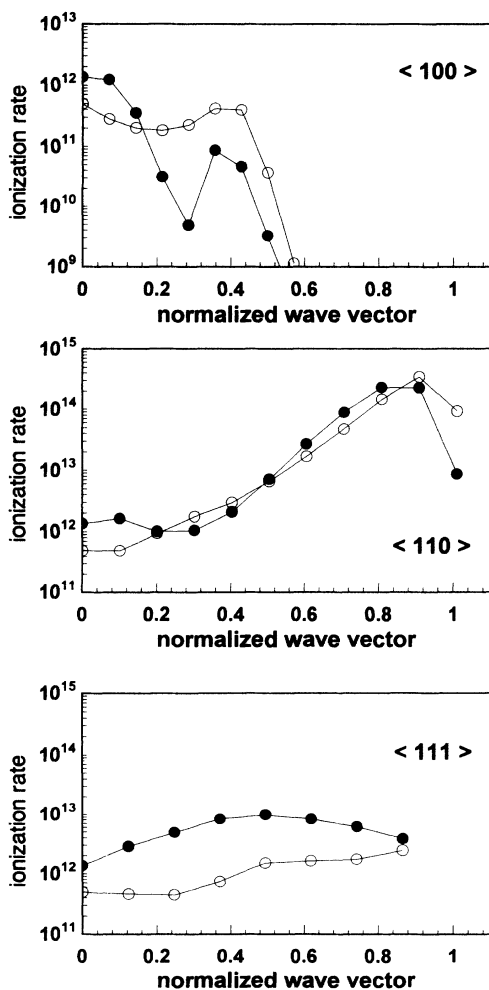


FIG. 4. Ionization rate for GaAs obtained from the numerical calculation for different band structures (Ref. 13: dots, Ref. 18: open circles) along the (a) $\langle 100 \rangle$, (b) $\langle 110 \rangle$, and (c) $\langle 111 \rangle$ directions.

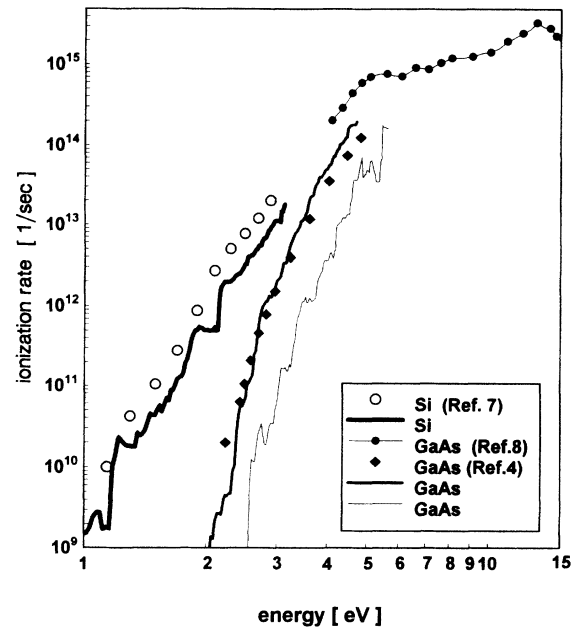


FIG. 5. Ionization rate for GaAs (Refs. 4, 8, and this work) and for Si (Ref. 7 and this work) vs energy measured from the conduction-band edge. The bold line for GaAs refers to a band structure of Ref. 13, the thin line to that of Ref. 18.

which are due to a complete numerical treatment of Eq. (1). An astonishing quantitative agreement can be noted, even if some deviations for all directions are apparent. The figures again show that the energy of the initial electron is the most important factor that almost uniquely determines the behavior of the ionization rate in \mathbf{k} space.

The similar representation of the correlation given by Sano and Yoshii for Si (Ref. 7) is founded on the Keldysh formula.¹⁰ Keldysh, however, expands the energies in the δ function near the threshold energy supposing *parabolic* bands. Especially for semiconductors like Si, this approximation is valid only in a formal way. Consequently, the functional correlation derived from our results is of the form x^4 rather than quadratic, as assumed in Ref. 7.

The correlation between the band structure and impact ionization rate refers to a very sensitive dependence of this quantity on the assumed energy dispersion. We studied this feature by applying another band structure to the calculation of the ionization rate. We have used the set of local pseudopotential parameters given by Humphries and Srivastava¹⁸ as the alternative one.

The results are shown in Fig. 4, together with those obtained by using the band structure of Ref. 13. Especially in $\langle 100 \rangle$ and $\langle 111 \rangle$ directions, large differences between the curves have to be noted. They result from a slightly different dispersion of the conduction bands. Since the ionization rate behaves obviously very sensitively with respect to the band structure in any case, the most realistic case has to be taken into account. Improved band structures as given, e.g., by nonlocal approaches¹⁹ may be the way to obtain more reliable results for the ionization rate.

Finally, the averaged ionization rate $R(E)$ for GaAs is shown in Fig. 5 compared to previous results given by Refs. 4 and 8, as well as to the ionization rate for Si. The results for GaAs calculated here were obtained with regard to the lowest three conduction bands for the initial electrons. For comparison with Ref. 7, we have considered only initial electrons belonging to the lowest conduction band in the case of Si.

First, we want to mention the main differences between the former treatment of the impact ionization rate in Ref. 8 and the present calculation. The former results⁸ were calculated using a simpler screening function for the interaction of conduction and valence electrons (the corrected Thomas-Fermi potential) and another approximation for the energy-conserving δ function. The results are distinguishable with respect to the general magnitude of the impact ionization rate as well as the threshold behavior. The absolute values for the impact ionization rate are determined mainly by the interaction strength of the electrons in the bands which itself is determined by the screening function. The improved screening function of Levine and Louie,¹⁵ especially its q dependence, yields a more realistic description of impact ionization processes compared to our previous calculation.

Additionally, the replacement of the energy δ function by a Lorentz profile, as favored in our previous paper,⁸ counts *all* combinations of \mathbf{k} values as ionization events with a specific weight, and thus causes a softening of the threshold behavior. It is obvious how the more reliable behavior near the threshold passes into the high-energy behavior already obtained in our former calculation.⁸

Comparison with the result of Bude and Hess⁴ for GaAs (see Fig. 5) reveals only a slightly softer threshold for their data. However, it shows a good overall agreement for the energy dependence of the ionization rate determined by different independent methods, i.e., a deterministic integration scheme and a Monte Carlo technique.

Furthermore, the ionization rate obtained with the alternative band structure of Ref. 18 is presented. Regarding the threshold behavior of both ionization rates for GaAs, the strong influence according to the different band structure is again visible and, as a result, the threshold energy differs by about $\Delta E_{\text{Th}} \approx 0.4$ eV. Besides the above-mentioned correlation between the energy of the initial electron and the ionization rate, a shift of the conduction bands to higher energies as caused, e.g., by a different band structure, leads to a smaller ionization rate. This is due to the decreasing ability of an electron with a given initial energy to occupy final states at those higher energies.

Comparing with the curves for Si and, especially, looking at the threshold behavior, the ionization rate in GaAs shows a rather steep increase. This is caused mainly by the stronger increase of the density of states in GaAs near the threshold energy compared to that of Si. The greater threshold energy for GaAs is simply a result of the larger gap energy in that material. Thus GaAs shows a harder threshold behavior than Si.

In addition, we compare the results for Si with those of

Sano and Yoshii (Ref. 7). The reason for the slight deviation between our results for Si and those of Ref. 7 is eventually due to small differences in the band structures, because all other effects were treated in the same way. In an extra calculation, the screening of the Coulomb interaction between the electrons in Si was treated by inserting the fit formula of Nara and Morita.²⁰ However, the slight differences in q dependence compared to the model function given by Levine and Louie¹⁵ have no notable influence on the results for the ionization rate.

IV. CONCLUSIONS

The anisotropy of the microscopic ionization rate in GaAs is strongly correlated with the band structure as well as the initial electron energy. Plotting the ionization rate in \mathbf{k} space versus the corresponding energy values given by the band structure reveals the unique dependence and leads to a simple general fit formula. The impact ionization rate can be calculated easily via this relation for all \mathbf{k} values, avoiding expensive numerical evaluations.

The band structure is the dominant input into the extensive numerical calculations, and the ionization rate behaves very sensitively with respect to the energy dispersion. This is shown clearly using slightly different band structures, which causes strong deviations in the behavior of the ionization rate along the symmetry lines in \mathbf{k} space.

Local pseudopotential band-structure data were used for calculating the ionization rate. However, they also determine the accuracy of the results for the ionization rate within the given method. The desirable application of a nonlocal band structure may lead to more rigorous results for the impact ionization rate. Studying the threshold behavior of the impact ionization rate, we could confirm that GaAs reveals features of a hard threshold, whereas Si has a much softer threshold behavior as a function of energy.

In our present calculations we have neglected phonon-assisted impact ionization processes, as well as deep-level ionization which may become of importance at high fields. Furthermore, other high-field effects such as collision broadening or the intracollisional field effect have to be considered for a more comprehensive description of the transport process of hot electrons in semiconductors similar to that in Ref. 5.

The aim of further calculations may be the study of the influence of the obtained anisotropy effects on the ionization coefficient, where an additional effect of the band structure is expected.²¹

ACKNOWLEDGMENTS

M.S. would like to thank Harold Eckstein for helpful and stimulating discussions. R.R. would like to thank the Department of Physics at Oregon State University for its kind hospitality during that period when this work was done, and the Alexander von Humboldt Stiftung for financial support.

- ¹C. Canali, C. Jacoboni, F. Nava, G. Ottaviani, and A. Alberigi-Quaranta, *Phys. Rev. B* **12**, 2265 (1975).
- ²T. P. Pearsall, R. E. Nahorny, and J. R. Chelikowsky, *Phys. Rev. Lett.* **39**, 292 (1977); T. P. Pearsall, F. Capasso, R. E. Nahorny, M. A. Pollack, and J. R. Chelikowsky, *Solid-State Electron.* **21**, 297 (1978); F. Capasso, R. E. Nahorny, M. A. Pollack, and T. P. Pearsall, *Phys. Rev. Lett.* **39**, 723 (1977); F. Capasso, R. E. Nahorny, and M. A. Pollack, *Electron. Lett.* **15**, 117 (1979).
- ³G. E. Bulman, V. M. Robbins, and G. E. Stillman, *IEEE Trans. Electron Devices* **ED-32**, 2454 (1985).
- ⁴J. Bude and K. Hess, *J. Appl. Phys.* **72**, 3554 (1992).
- ⁵J. Bude, K. Hess, and G. J. Iafrate, *Phys. Rev. B* **45**, 10958 (1992).
- ⁶Y. Wang and K. Brennan, *J. Appl. Phys.* **71**, 2736 (1992).
- ⁷N. Sano and A. Yoshii, *Phys. Rev. B* **45**, 4171 (1992).
- ⁸M. Stobbe, A. Könies, R. Redmer, J. Henk, and W. Schattke, *Phys. Rev. B* **44**, 11105 (1991).
- ⁹E. O. Kane, *Phys. Rev.* **159**, 624 (1967).
- ¹⁰L. V. Keldysh, *Zh. Eksp. Teor. Fiz.* **37**, 713 (1959) [*Sov. Phys. JETP* **10**, 509 (1960)].
- ¹¹The analytical approaches are reviewed by D. J. Robbins, *Phys. Status Solidi B* **97**, 9 (1980); **97**, 387 (1980); **98**, 11 (1980).
- ¹²A. Baldereschi, *Phys. Rev. B* **7**, 5212 (1973); D. J. Chadi and M. L. Cohen, *ibid.* **8**, 5747 (1973); H. J. Monkhorst and J. D. Pack, *ibid.* **13**, 5188 (1976).
- ¹³M. L. Cohen and T. K. Bergstresser, *Phys. Rev.* **141**, 789 (1966).
- ¹⁴D. B. Laks, G. F. Neumark, A. Hangleiter, and S. T. Pantelides, *Phys. Rev. Lett.* **61**, 1229 (1988).
- ¹⁵Z. H. Levine and S. G. Louie, *Phys. Rev. B* **25**, 6310 (1982). See also M. S. Hybertson and S. G. Louie, *Phys. Rev. Lett.* **55**, 1418 (1985); *Phys. Rev. B* **34**, 5390 (1986).
- ¹⁶S. B. Zhang, D. Tomanek, M. L. Cohen, S. G. Louie, and M. S. Hybertson, *Phys. Rev. B* **40**, 3162 (1982); X. Zhu and S. G. Louie, *ibid.* **43**, 14142 (1991).
- ¹⁷P.-O. Löwdin, *J. Chem. Phys.* **19**, 1396 (1951).
- ¹⁸T. P. Humphreys and G. P. Srivastava, *Phys. Status Solidi B* **112**, 581 (1982).
- ¹⁹J. R. Chelikowsky and M. L. Cohen, *Phys. Rev. B* **14**, 556 (1976).
- ²⁰H. Nara and A. Morita, *J. Phys. Soc. Jpn.* **21**, 1852 (1966).
- ²¹K. Kim, K. Kahen, J. P. Leburton, and K. Hess, *J. Appl. Phys.* **59**, 2595 (1986).